Journal of Power Sources 256 (2014) 354–360

Contents lists available at ScienceDirect

Journal of Power Sources

journal homepage: www.elsevier.com/locate/jpowsour

In situ electrodeposition of graphene/nano-palladium on carbon cloth for electrooxidation of methanol in alkaline media

A. Safavi [a,b,*], H. Kazemi [a], S.H. Kazemi [c,d]

[a] Department of Chemistry, College of Sciences, Shiraz University, Shiraz, Iran
[b] Nanotechnology Research Institute, Shiraz University, Shiraz, Iran
[c] Department of Chemistry, Institute for Advanced Studies in Basic Sciences (IASBS), Zanjan 45137-66731, Iran
[d] Center for Research in Climate Change and Global Warming (CRCC), Institute for Advanced Studies in Basic Sciences (IASBS), Zanjan 45137-66731, Iran

HIGHLIGHTS

- In-situ electrodeposition of graphene–Pd nanocomposite was achieved on a cheap carbon cloth.
- Well-dispersed Pd was obtained by this facile method.
- This nanocatalyst exhibits high electrocatalytic activity and stability for methanol oxidation.
- Excellent tolerance toward electrode poisoning was observed in alkaline media.

ARTICLE INFO

Article history:
Received 9 August 2013
Received in revised form
17 November 2013
Accepted 3 December 2013
Available online 22 January 2014

Keywords:
Electrodeposition
Graphene nano-palladium composite
Carbon cloth
Methanol oxidation

ABSTRACT

Electrocatalytic oxidation of methanol in alkaline medium is studied using graphene nano-palladium/carbon cloth (G-Pd/CC). X-ray diffraction, scanning electron microscopy (SEM) and atomic absorption spectrometry are used to characterize G-Pd/CC electrode. Electrochemical characterizations are performed using cyclic voltammetry (CV), chronoamperometry and electrochemical impedance spectroscopy (EIS). The results show that the application of CC as a substrate for G-pd reveals excellent characteristics such as high catalytic activity, stability, tolerance toward poisoning effects for electrooxidation of methanol in alkaline medium. All results show that this electrode is a good candidate for application in direct methanol fuel cells.

1. Introduction

Direct liquid fuel cells, such as direct alcohol fuel cells (DAFCs) have attracted much attention as one of the most viable candidates to replace batteries as a source of portable power [1,2]. Methanol and ethanol are popular alternative fuels for DAFCs. Methanol has higher theoretical energy density than other alcohols and is miscible with water [2].

Among the electrocatalysts for alcohols oxidation, Pt and Pt-based alloys have been extensively investigated [3]. However, some challenges such as the cost of Pt or Pt-based electrocatalysts, slow reaction kinetics and electrode poisoning by CO like intermediates which are formed in the alcohol oxidation reaction still remain as problems in using Pt-based catalysts. To overcome such problems, Pt-free electrocatalysts were developed. Among these materials, Pd-based catalysts are less expensive and have a comparable or even better electrocatalytic activities than Pt-based catalysts for alcohol oxidation [4,5].

Although Pd itself has been proven to be a suitable catalyst for electrooxidation of alcohols in alkaline media, more efforts are needed for further improvement of electrocatalytic performance of Pd-based catalysts. Supporting on materials with large surface areas such as carbon black, activated carbon, carbon nanofibers and carbon nanotube [4–6] is one approach. Graphene, as a new carbon nanomaterial with two-dimensional lattice made of sp^2 hybridized carbon atoms, has recently attracted great attention due to its unique electrical, optical, and mechanical properties [7,8]. These unique properties yield potential for applications in energy conversion and storage systems such as fuel cells, batteries, supercapacitors, sensors and solar cells. Many methods have been proposed for graphene production [7,9]. Among these methods,

* Corresponding author. Department of Chemistry, College of Sciences, Shiraz University, Shiraz, Iran.
E-mail addresses: afsaneh_safavi@yahoo.com, safavi@chem.susc.ac.ir (A. Safavi).

0378-7753/$ – see front matter © 2014 Elsevier B.V. All rights reserved.
http://dx.doi.org/10.1016/j.jpowsour.2013.12.139

electrochemical reduction of graphene oxide (GO) has been attractive because it is simple, fast, and green [7]. Chen et al. showed that GO in solution can be electrochemically reduced to yield graphene on a glassy carbon electrode (GCE) surface [10]. Also, Jiang et al. reported one-step co-electrodeposition of graphene/Pd composite film on the GCE for formic acid electrooxidation [11]. This method is a one-step, simple and fast strategy for co-deposition of graphene and Pd [11] or graphene and Au [7]. In this method, nanoparticles are sandwiched between graphene sheets and a multilayer composite is formed [7]. Recently, a layer by layer Pt graphene is fabricated on the carbon fiber for electrooxidation of methanol [12]. The layer by layer structure exhibits greatly enhanced catalytic activity toward methanol electrooxidation. However, the fabrication method is complicated and has several steps [12].

In the present study, the use of carbon cloth, which has been widely used in fuel cells as current collector due to its good conductivity, high stability and commercial availability, is described as a substrate for fabrication of a graphene-nanoPd/carbon cloth (G-Pd/CC) [11]. Here, graphene and nano-Pd were deposited in situ on CC. The electrocatalytic behavior of the G-Pd/CC is investigated toward methanol electrooxidation in alkaline media. The results show that the G-Pd/CC provides high electrocatalytic activity and good tolerance toward poisoning species for methanol oxidation reaction in an alkaline media. The electrochemical behaviors of this electrode are investigated using cyclic voltammetry (CV), chronoamperometry and electrochemical impedance spectroscopy (EIS).

2. Experimental

2.1. Reagents and apparatus

The graphene oxide (GO) was synthesized by the modified Hummers' method [13]. All chemicals were analytical grade. All electrochemical measurements were carried out using a potentiostat/galvanostat (PGSTAT302) equipped with FRA board for EIS measurements. A three electrode cell containing G-Pd/CC(CC was purchased from E-TEK, 3.6 cm^2) as working electrode, platinum disk as the counter electrode and SCE electrode as the reference electrode was used. CC was used as a substrate for deposition of G-nanoPd. One side of CC was covered with Teflon paper and the electric contact was established via a copper wire. G-Pd composite, was electrodeposited in situ on the CC using a similar method described elsewhere [11]. Briefly, the repetitive cyclic voltammetry (CV, 10 cycles) scanning were carried out from −1.5 V to 0.6 V at 25 mV s^{-1} in a phosphate buffer solution (PBS 0.067M, pH 9.18) containing 0.6 mg mL^{-1} GO and 1 mM palladium chloride (with magnetic stirring and N_2 bubbling). For comparison, Pd/CC electrode was prepared by electrodeposition under the same conditions without the addition of GO. GO was deposited in the same way without the addition of palladium salt in the electrolyte. The electrolyte used for electrochemical characterization of the prepared electrode was 1 M KOH and cyclic voltammograms were recorded at a scan rate of 50 mV s^{-1}. The electrolyte solution was deaerated with pure nitrogen for about 10 min prior to each experiment. EIS measurements were carried out from 100 KHz to 10 mHz with a 10 mV Ac amplitude. EIS results were analyzed by using ZMan 2.0 software (ZAHNER-Elektrik GmbH & Co. KG). Scanning electron micrographs (SEM) of the electrode surfaces were obtained by using scanning electron microscopy (Hitachi S-41 field emission SEM (FESEM), model XL30) at an accelerating voltage of 25 kV. Also, the size of the Pd nanoparticles on the graphene nano sheets was evaluated by transmission electron microscopy (TEM, Zeiss, EM10C, 80 KV). Pd loading on the modified electrode was determined by atomic absorption spectrometry (Varian Model SpectrAA 220 (Mulgrave, Vic., Australia).

3. Results and discussion

3.1. Characteristics of G-Pd/CC composite

Fig. 1A shows SEM image of bare CC. The SEM image of reduced GO is shown in Fig. 1B. A typical wrinkled sheet structure of graphene is observed that provides a substrate with large rough surface for nanoparticles modification. A similar morphology has been reported previously [10]. The average size of the Pd nanoparticles on the graphene nano sheets were evaluated from TEM images (Fig. 2D, E, F) and found to be about 8 nm. Also, as shown in Fig 2, Pd nanoparticles can be observed under the graphene sheets. This is because the deposition of Pd nanoparticles was started before deposition of graphene during cathodic scans and yielding a layer of Pd nanoparticles [7]. Then in the high enough cathodic potential (>−1.0 V), GO reduction was occurred and covered the Pd nanoparticles [7,10]. This event repeated several time during cyclic voltammetric scans and led to the formation of multi layered Pd and graphene [7]. Also, as shown in Fig. 2, the nanoparticles of Pd are dispersed homogenously and are not aggregated compared to the case when only Pd is electrodeposited on the CC (Fig. 1C). This may be attributed to the strong anchoring effect between Pd nanoparticles and the graphene surface, which prevents aggregation of the NPs [7,12]. As previously confirmed, the remaining oxygen-containing groups on the reduced GO could provide binding sites for anchoring precursor metal ions or metal nanoparticles [12,14]. Also, aggregation of graphene sheet was prevented when Pd nanoparticles lied between graphene layers and consequently enhanced surface area of G-Pd composite [7]. The EDX spectrum of G-Pd/CC electrode shown in Fig. 1D consists of a sharp peak at 0.28 keV associated with C Kα due to the carbon atoms of G and CC, and a predominant peak at 2.84 keV from Pd $L\alpha_1$ due to the Pd element [15].

The amount of Pd loading on graphene nanosheets was determined using atomic absorption spectrometry after dissolution of Pd nanoparticles in aqua regia. The Pd loading values for G-Pd/CC and Pd/CC were 0.35 mg and 0.19 mg, respectively. The larger capacity for Pd loading in the G-Pd structure may be attributed to larger surface area of graphene and formation of multi layered structure in this case.

3.2. Voltammetric studies

Fig. 3 shows voltammetric data illustrating the growth of Pd and G-Pd on the CC. As clearly observed, for electrodeposition of G-Pd, the reductive peak current (lower than −1.0 V) increased larger than those in the Pd reduction which indicates that co-deposition of graphene and Pd has been occurred [11].

Fig. 4 shows the cyclic voltammograms (CVs) of 1 M KOH solution (blank solution) at Pd/CC and G-Pd/CC electrodes. As shown in this figure, two regions can be observed. In the first region, between −1.0 and −0.6 V, two well-defined anodic peaks (−0.9 and −0.65 V) and one cathodic peak (−0.9 V) corresponding to the hydrogen adsorption and desorption are observed, respectively [16]. In the second region, between −0.6 and 0.4, a plateau region-type feature (approximately between −0.40 V and 0.40 V) in the positive scan is attributed to the oxidation of Pd and a strong reduction peak (between −0.4 and −0.6 V) in cathodic scan is the characteristic peak for the reduction of PdO_x [17,18]. It should be pointed out that the hydrogen adsorption, desorption for Pd/CC electrodes only form one pair of peaks. Moreover, the current of the G-Pd/CC electrode is much larger than that at the Pd/CC electrode,

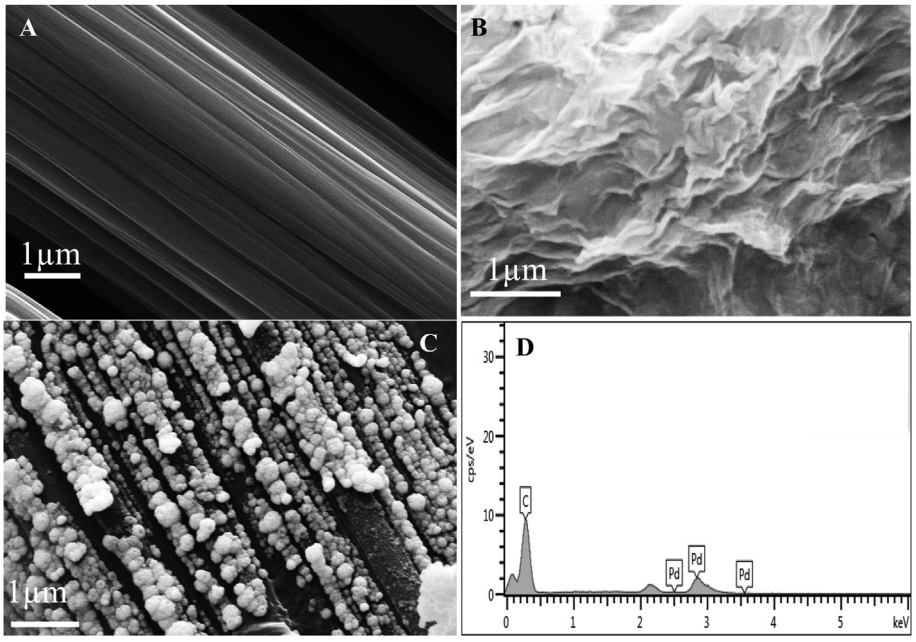

Fig. 1. FESEM images of CC (A), G/CC (B), Pd/CC (C), and EDX spectrum of G-Pd/CC (D).

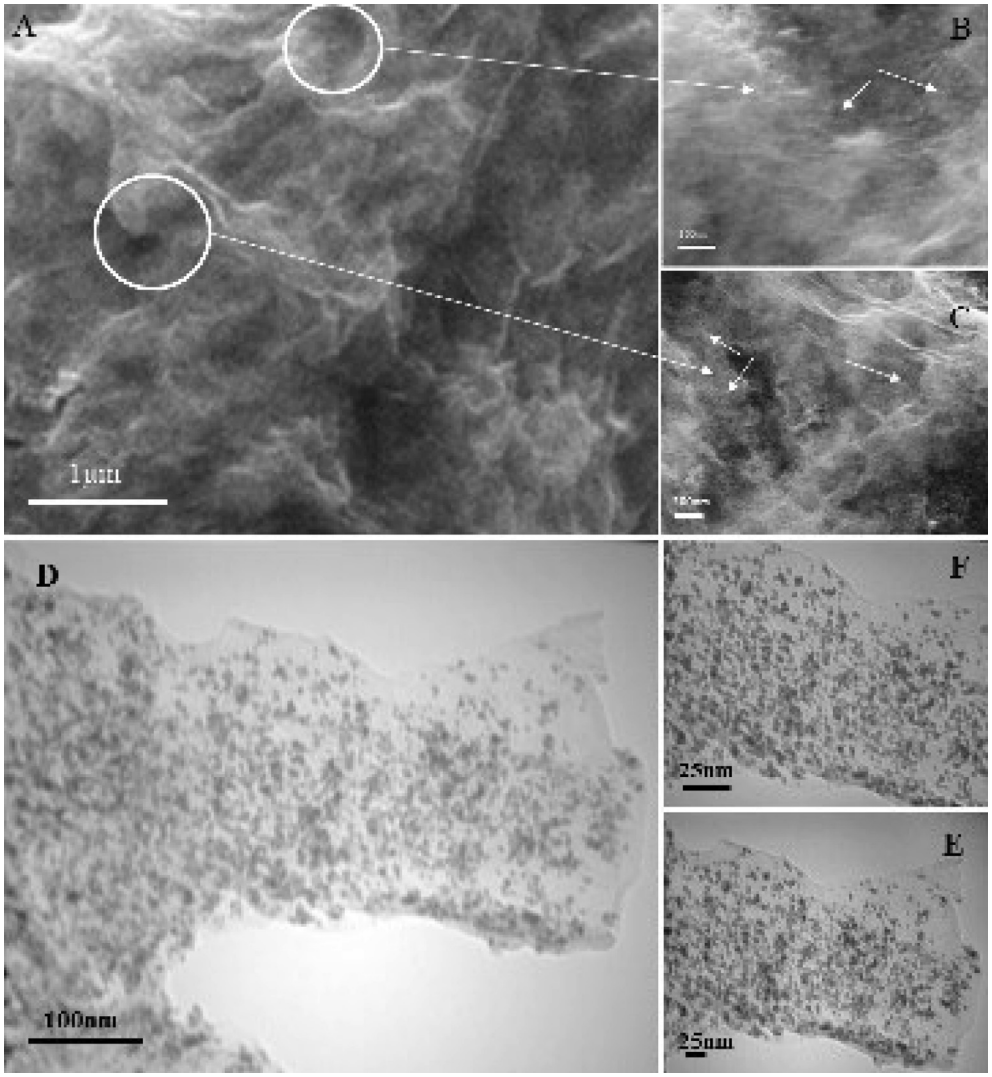

Fig. 2. FESEM images of, G-Pd/CC (A), higher magnification of G-Pd/CC (B, C), TEM images of, G-Pd/CC (D), higher magnification of G-Pd/CC (E, F).

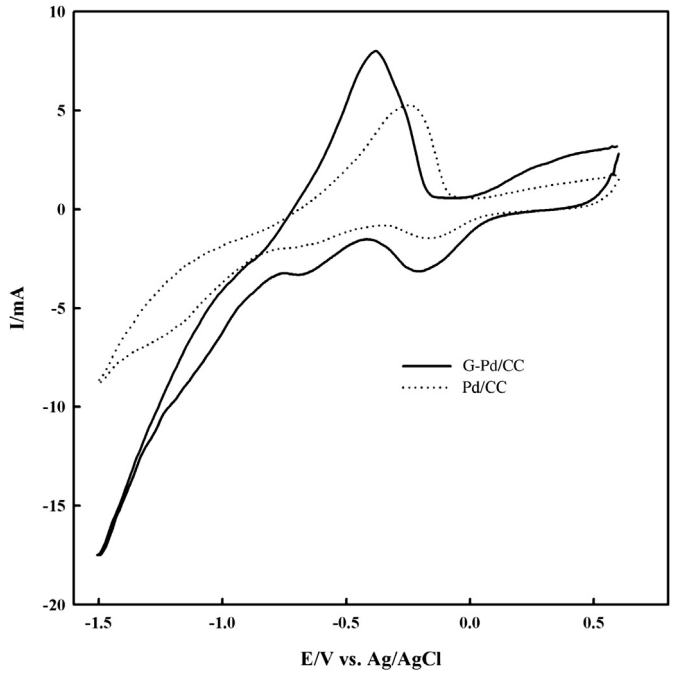

Fig. 3. Tenth cycle in electrodeposition process of G-Pd/CC and Pd/CC by cycling potential from 0.6 to −1.5 V at 25 mV s^{-1}.

which is due to the large surface area of separated Pd nanoparticles. This is very favorable for the application of nanomaterials as electrocatalysts [16,19].

The electrochemical active surface area (ECSA) was determined using the charge associated with the surface oxide reduction peak by assuming formation of a monolayer of PdO on Pd [20]. The ECSAs of G-Pd/CC and Pd/CC are 24.2 cm^2 and 7.8 cm^2, respectively. It is evident that the ECSA of the metal catalyst is largely improved (3 times) when Pd is co-deposited with graphene as compared to Pd deposition alone. This is due to the fact that, aggregation of Pd NPs on the surface of graphene is prevented because of the strong anchoring effect between the Pd nuclei and graphene sheets [7,12].

Electrooxidation activity of Pd/CC and G-Pd/CC toward methanol was investigated in a solution containing 1 M KOH and 1 M CH_3OH (Fig. 5). G-Pd/CC showed higher (9 time) electrocatalytic activity than that of the Pd/CC. However, the oxidation peak potential on G-Pd/CC (0.3 V) was more positive than that at Pd/CC (−0.15 V). This indicates that graphene inhibits oxidation of Pd until more positive potentials are reached and electrooxidation of methanol occurred in the larger potential range.

The onset potential is an important parameter to characterize the activity of methanol electrooxidation on an electrocatalyst [4]. From the CV curves (Fig. 5), it is revealed that the onset potentials for the oxidation of methanol on the G-Pd/CC and Pd/CC are about −0.63 and −0.35 V, (vs. SCE), respectively. The onset potential for the methanol oxidation on the G-Pd/CC electrode is 280 mV more negative than that observed on the Pd/CC electrode, indicating enhancement in the kinetics of the methanol oxidation reaction.

Another parameter that is often taken as a benchmark of the performance of a catalyst is the ratio of the forward peak current (I_f) to the backward peak current (I_b). Larger I_f/I_b value indicates higher catalytic efficiency and better tolerance towards the poisoning species arising from the formation of the carbonaceous intermediate on the catalyst during the reaction [21,22]. The I_f/I_b value of G-Pd/CC electrode is 5.8, which is much larger than that of Pd/CC electrode (2.5). This again indicates that G-Pd/CC has better poisoning-tolerant behavior and catalytic efficiency. This value is higher than most of the previously reported values for Pd-based electrocatalysts for methanol oxidation reaction in alkaline media.

3.3. Chronoamperometric analysis

In order to further evaluate the activity and stability of methanol electrooxidation, chronoamperometric tests were performed at a fixed potential of −0.1 V in a 1.0 M KOH solution containing 1.0 M

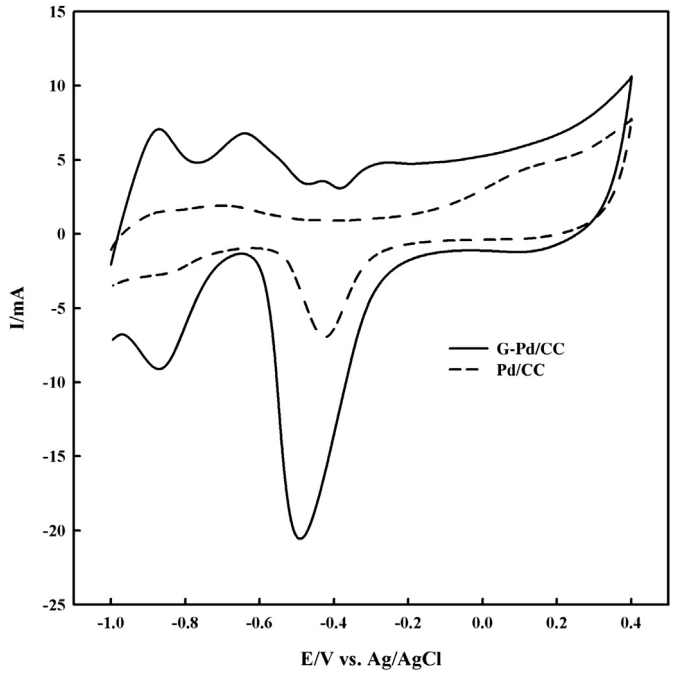

Fig. 4. Cyclic voltammograms of Pd-G/CC and Pd/CC electrodes in 1 M KOH at a scan rate of 50 mV s^{-1}.

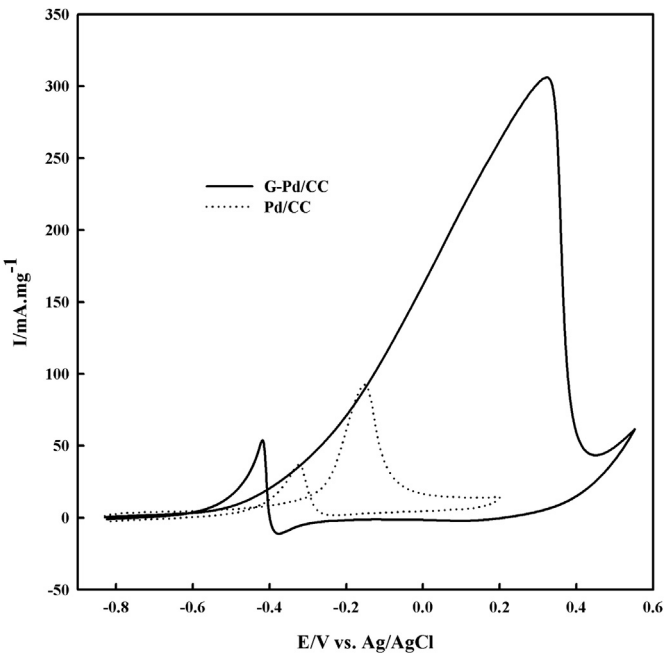

Fig. 5. Cyclic voltammograms of Pd-G/CC and Pd/CC electrodes in 1 M KOH and 1 M methanol at a scan rate of 50 mV s^{-1}.

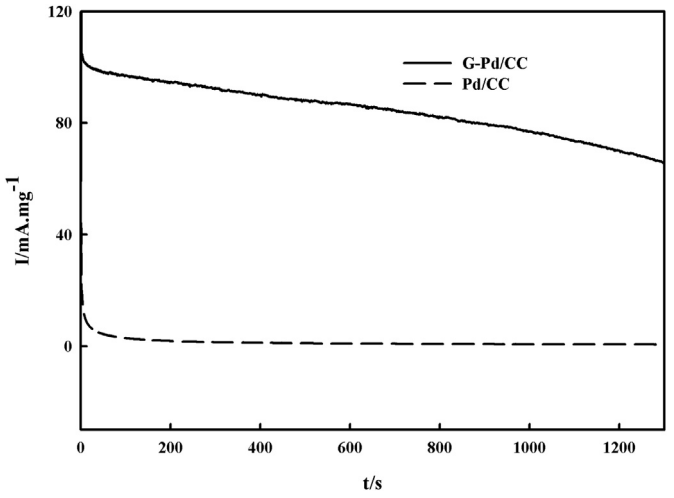

Fig. 6. Chronoamperometric results of the G-Pd/CC and Pd/CC electrodes in 1 M KOH containing 1 M methanol solution at a working potential of −0.1 V (vs SCE).

methanol. As is shown in Fig. 6, the current density on G-Pd/CC was considerably higher than that on Pd/CC. All these results confirmed that the G-Pd/CC has better catalytic activity and stability than Pd/CC toward the oxidation of methanol in an alkaline media [23]. An improved tolerance to the poisoning species, catalytic activity and stability of the G-Pd/CC may be attributed to several layer structure of G-Pd on the CC. This structural effect has been also reported previously [7,12].

3.4. Electrochemical impedance studies of methanol electrooxidation at G-Pd/CC electrode

Electrochemical impedance spectroscopy (EIS) was used to investigate the electron transfer kinetics of methanol oxidation reaction on G-Pd/CC in different potential ranges. The measurements were made in 1 M methanol solution containing 1 M KOH and the electrode potentials were scanned every 0.05 V from −0.65–0.40 V. As shown in Fig. 7, in the low potential region ($E < -550$ mV), the Nyquist plot is characterized by a capacitive feature, attributed to double layer charging/discharging

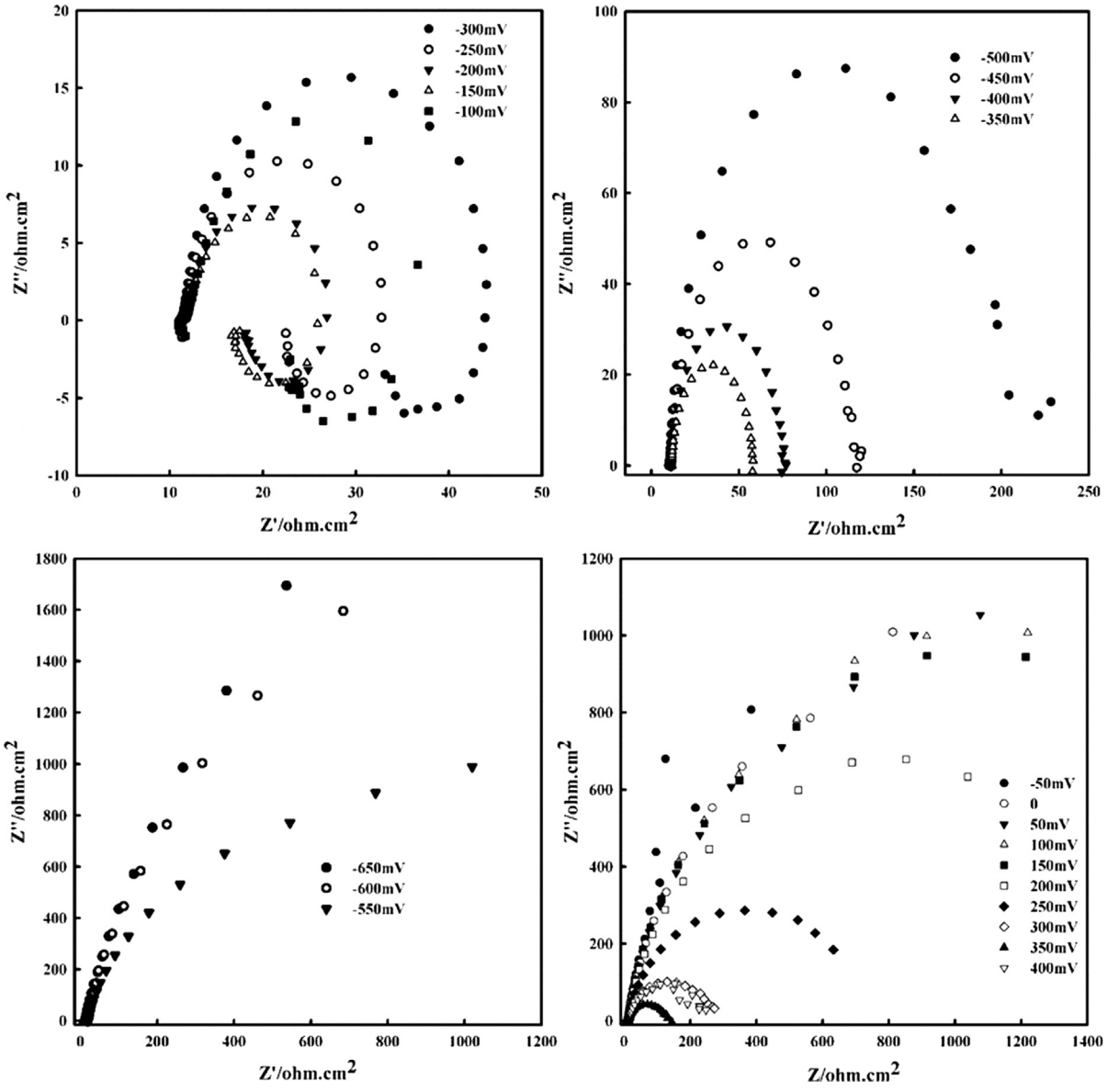

Fig. 7. Nyquist plots of the ethanol oxidation on the Pd-G/CC electrode in 1 M KOH containing 1 M methanol at different electrode potentials (every 0.05 V from −0.65 to 0.4 V).

phenomena and hydrogen adsorption/desorption [24]. In the potential range between −500 and −350 mV, capacitive semicircles are observed, indicating a slow reaction rate of methanol oxidation [24,25]. In higher potential region (−300 to −100 mV), there is a transition from capacitive behavior to resistive behavior [24]. Each impedance curve in this region has three distinct parts. A small arc at high frequencies is attributed to chemisorptions and dehydrogenation of the methanol molecule at the beginning of the oxidation process [20,24]. A relatively large semicircle at intermediate frequencies is related to the charge transfer reaction kinetics. The diameter of this semicircle decreases with increasing potential, indicating faster reaction kinetics at higher anodic potentials [20]. A smaller loop in the fourth quadrant (inductive loop) at low frequencies may be ascribed to the formation and adsorption of CO intermediate species on the electrode surface in this region [26]. As potential increases in this region, the diameter of the low frequency inductive loop decreases. This can be related to the enhanced desorption of adsorbed CO intermediate at the electrode surface, particularly at higher potentials [16]. At higher potentials, the weakly-bonded CO will be oxidized, leading to the recovery of the surface reaction sites and hence, increase in the rate of methanol oxidation reaction [20]. In the potentials more positive than −50 mV, the impedance plots return to normal behaviors. In this region, the diameter of the arc decreases from 100 to 350 mV, because of faster electron transfer at higher potentials and then increases thereafter. The later part (>350 mV) is attributed to the formation of palladium oxide. As expected palladium oxide is not active toward methanol oxidation [27]. For better understanding the ac impedance behavior, EIS results were fitted by using two appropriate equivalent circuits shown in Scheme 1 [25]. In Scheme 1, circuit A was applied for fitting all EIS results except the potentials in which the inductive loop was observed. To take into account of inductive behavior, circuit B was used. It should be noted that in Scheme 1, R_s is the solution resistance, R_{ct} is the charge−transfer resistance, CPE_{dl} (or Q_{dl}) is the constant phase element corresponding to the double layer capacitance and CPE_{ads} (or Q_{ads}) and R_{ads} are the electrical elements related to the adsorption of methanol on the electrode surface. Also, in circuit B of Scheme 1, L is representative for inductance of the adsorbed layer and R_3 is the inverse of the rate constant of the process of the regeneration of active sites for the adsorption and oxidation of methanol [25]. Tables 1and 2 represent the electrochemical parameters obtained for G-Pd/CC electrode estimated from equivalent circuit fitting. In addition, to compare the effect of graphene on the electrode

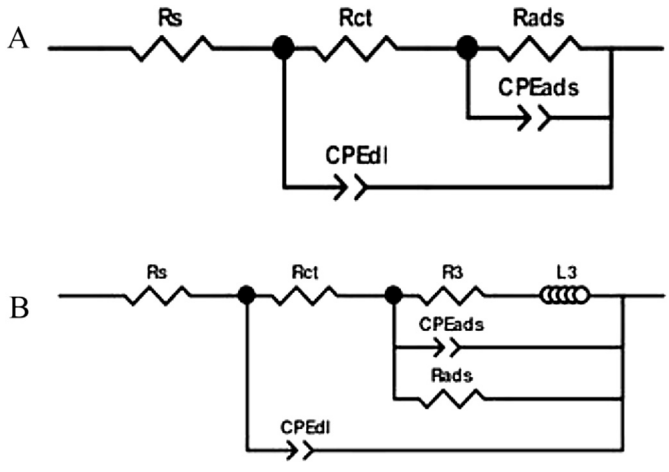

Scheme 1. The equivalent circuits for the impedance spectra A) without and B) with inductive behavior.

Table 1
Electrical parameters estimated for EIS results of G-Pd/CC electrode using circuit A in Scheme 1.

E/mV	R_{ads}	C_{ads}/F	R_{ct}	C_{dl}/F
−650	555.86	0.00874	628.65	0.00212
−550	171.23	0.00751	176.01	0.00404
−500	171.23	0.00751	176.01	0.00404
−350	71.25	0.00644	85.29	0.00078
−200	40.25	0.00588	67.09	0.03364
−150	130.54	0.00795	8.21	0.12277
−100	363.60	0.01149	76.88	0.08069
−50	333.86	0.00821	338.84	0.03279
0	379.61	0.00668	104.90	0.03788
50	361.53	0.00675	128.46	0.02796
100	361.53	0.00675	128.46	0.02796
150	294.19	0.00636	315.90	0.02403
200	262.22	0.00646	267.69	0.05329
250	158.26	0.00526	68.24	0.03526
300	110.97	0.00508	12.12	0.20841
350	74.38	0.00450	6.79	0.30340
400	363.60	0.01149	76.88	0.08069

behavior, the electrochemical impedance spectra were analyzed for Pd/CC electrode using the same circuits (Tables 3 and 4). It can be seen that the charge transfer kinetics at G-Pd/CC electrode is relatively faster than at Pd/CC surface, especially in the potential region of −200 to +400 mV in which the electrooxidation process is occurred. Also, R_3 parameters for both G-Pd/CC and Pd/CC electrodes decreased by increasing the potential towards the anodic direction which means that the rate of the regeneration of active sites at the surface of both electrodes will be increased by increasing potential. EIS results reveal that the G-Pd/CC electrode can be considered as a good alternative for anode electrode in direct methanol fuel cells.

4. Conclusions

G-nanoPd was electrodeposited in situ on a CC as a substrate for fabrication of a graphene-Pd/carbon cloth (G-Pd/CC). CC has been widely used in fuel cells as a current collector due to its good

Table 2
Electrical parameters estimated for EIS results of G-Pd/CC electrode using circuit B in Scheme 1.

E/mV	R_{ads}/ohm	C_{ads}/F	R_{ct}/ohm	C_{dl}/F	R_3	L
−300	0.91	0.03	32.7	0.00185	47.5	162.0
−250	1.17	0.079	21.2	0.0019	19.0	25.0
−200	0.88	0.037	15.8	0.0021	10.2	7.0
−150	1.1	0.03	14.7	0.0030	6.0	2.9
−100	2.1	0.021	28.0	0.0026	9.8	3.3

Table 3
Electrical parameters estimated for EIS results of Pd/CC electrode using circuit A in Scheme 1.

E/mV	R_{ads}	C_{ads}/F	R_{ct}	C_{dl}/F
−500	191.0	0.00190	8.8	0.21592
−400	43.3	0.00174	48.5	0.028
−350	37.2	0.00168	62.8	0.094
−200	6.8	0.00162	101.0	0.077
−150	5.2	0.00181	101.0	0.092
−50	946.0	0.00367	968.0	0.075
0	2350.0	0.00347	1190.0	0.0002
100	1030.0	0.00237	1400.0	0.126
150	965.0	0.00236	1290.0	0.00003
200	812.0	0.00238	832.0	0.00010
250	366.0	0.00206	339.0	0.00004
300	131.0	0.00208	130.0	0.00154

Table 4
Electrical parameters estimated for EIS results of Pd/CC electrode using circuit B in Scheme 1.

E/mV	R_{ads}/ohm	C_{ads}/F	R_{ct}/ohm	C_{dl}/F	R_3	L
−300	0.91	0.031	32.7	0.00186	47.5	162.3
−250	1.41	0.11	21.2	0.00192	18.9	24.1

conductivity, high stability and commercial availability. SEM and TEM images show that the presence of graphene prevents aggregation of Pd nanoparticles. The electrochemical results show that the electrode reveals excellent characteristics such as high catalytic activity, and high tolerance toward poisoning effects for electrooxidation of methanol in alkaline medium. Larger I_f/I_b value for G-Pd/CC electrode indicates higher catalytic efficiency and good tolerance toward electrode poisoning in alkaline media. Also, the large increase in current of G-Pd/CC electrode compared to Pd/CC is due to high surface area attributed to the presence of graphene. All results show that this electrode is a good candidate for application in direct methanol fuel cells.

Acknowledgments

The authors wish to express their gratitude to Iran's National Elites Foundation and Shiraz University Research Council for the support of this work.

References

[1] S.T. Nguyen, H.M. Law, H.T. Nguyen, N. Kristian, S. Wang, S.H. Chan, X. Wang, Appl. Catal. B 91 (2009) 507.
[2] F. Miao, B. Tao, Electrochim. Acta 56 (2011) 6709.
[3] F. Cheng, X. Dai, H. Wang, S.P. Jiang, M. Zhang, C. Xu, Electrochim. Acta 55 (2010) 2295.
[4] Z. Liu, B. Zhao, C. Guo, Y. Sun, Y. Shi, H. Yang, Z. Li, J. Colloid Interface Sci. 351 (2010) 233.
[5] Y.-H. Qin, H.-H. Yang, X.-S. Zhang, P. Li, X.-G. Zhou, L. Niu, W.-K. Yuan, Carbon 48 (2010) 3323.
[6] Y. Wang, Z. Min, H. Yang, S. Ping, C. Ming, Int. J. Hydrogen Energy 35 (2010) 10087.
[7] C. Liu, K. Wang, S. Luo, Y. Tang, L. Chen, Small 7 (2011) 1203.
[8] J. Liu, Y. Qiao, C.X. Guo, S. Lim, H. Song, C.M. Li, Bioresour. Technol. 114 (2012) 275.
[9] A. Safavi, M. Tohidi, F.A. Mahyari, H. Shahbaazi, J. Mater. Chem. 22 (2012) 3825.
[10] L. Chen, Y. Tang, K. Wang, C. Liu, S. Luo, Electrochem. Commun. 13 (2011) 133.
[11] Y. Jiang, Y. Lu, F. Li, T. Wu, L. Niu, W. Chen, Electrochem. Commun. 19 (2012) 21.
[12] Z. Yao, R. Yue, C. Zhai, F. Jiang, H. Wang, Y. Du, C. Wang, P. Yang, Int. J. Hydrogen Energy 38 (2013) 6368.
[13] W.S. Hummers, R.E. Offeman, J. Am. Chem. Soc. 80 (1958) 1339.
[14] Y. Li, L. Tang, J. Li, Electrochem. Commun. 11 (2009) 846.
[15] G. Hu, F. Nitze, H.R. Barzegar, T. Sharifi, A. Mikołajczuk, C.-W. Tai, A. Borodzinski, T. Wågberg, J. Power Sources 209 (2012) 236.
[16] Y. Lu, W. Chen, J. Phys. Chem. C 114 (2010) 21190.
[17] R. Awasthi, R.N. Singh, Int. J. Hydrogen Energy 37 (2012) 2103.
[18] G. Li, L. Jiang, Q. Jiang, S. Wang, G. Sun, Electrochim. Acta 56 (2011) 7703.
[19] S. Yang, X. Zhang, H. Mi, X. Ye, J. Power Sources 175 (2008) 26.
[20] R. Awasthi, R.N. Singh, Open Catal. J. 4 (2011) 100.
[21] L. Su, W. Jia, A. Schempf, Y. Ding, Y. Lei, J. Phys. Chem. C 113 (2009) 16174.
[22] L.D. Zhu, T.S. Zhao, J.B. Xu, Z.X. Liang, J. Power Sources 187 (2009) 80.
[23] L. Dai, L.-P. Jiang, E.S. Abdel-Halim, J.-J. Zhu, Electrochem. Commun. 13 (2011) 1525.
[24] S.S. Mahapatra, J. Datta, Int. J. Electrochem. 2011 (2011) 1.
[25] I. Danaee, M. Jafarian, F. Forouzandeh, F. Gobal, M. Mahjani, Int. J. Hydrogen Energy 34 (2009) 859.
[26] W. Chen, J. Kim, S. Sun, S. Chen, Langmuir 23 (2007) 11303.
[27] A. Safavi, H. Kazemi, S. Momeni, M. Tohidi, P. Khanipour Mehrin, Int. J. Hydrogen Energy 38 (2013) 3380.